OPEN ACCESS

International
Journal
Of Modern Engineering Research (IJMER)

A Combined Element Based Frequency Selective Surface for 60 GHz Millimeter-Wave WLAN Applications

Robson H. C. Maniçoba[1], Agnaldo V. Lovato[1], Marcelo A. Guimarães[1], Lucas S. de Oliveira[1]
Murilo S. Santana[1], Alex F. dos Santos[2], Alexandre M. de Oliveira[3], Karcius D. R. Assis[4]

[1]*DCT – CCSI – CPDS, State University of Southwest Bahia (UESB), Jequié – BA, Brazil*
[2]*CETENS, Federal University of Recôncavo da Bahia (UFRB), Feira de Santana – BA, Brazil*
[3]*LABMAX, Federal Institute of Education, Science and Technology of São Paulo, Suzano – SP, Brazil*
[4]*DEE, Federal University of Bahia (UFBA), Salvador – BA, Brazil*

ABSTRACT: *In this paper, a single-layer combined element based Frequency Selective Surface is proposed for 60 GHz Millimeter-Wave Wireless Local Area Networks (WLAN) Applications. The element geometry used in the unit cell for the proposed structure consists of a simple modification in the element obtained by the concept of simple combined element (SCE). The basic elements: square loop, cross- dipole and square patch were used to obtain this element. The results demonstrate a wide 11 GHz stopband in the 60 GHz WLAN (802.11 ad) frequency range.*

Keywords: *Frequency Selective Surface, Combined Element, WLAN, Millimeter-Wave*

I. INTRODUCTION

Frequency Selective Surfaces (FSS) are defined as periodic structures of identical elements arranged in two or three dimensions forming an infinite array. This array can be formed by all-dielectric elements, aperture type elements or conductive patch type elements, in a single or multilayer structure. FSS has electromagnetic properties, in terms of transmission and reflection characteristics, that vary with frequency. They can act as filters that operate on free-space waves, exhibit band-stop or bandpass characteristics, which depends primarily on the type and the geometry of the structure on one period called unit cell [1-3]. An example of this type of structure is shown in Fig. 1.

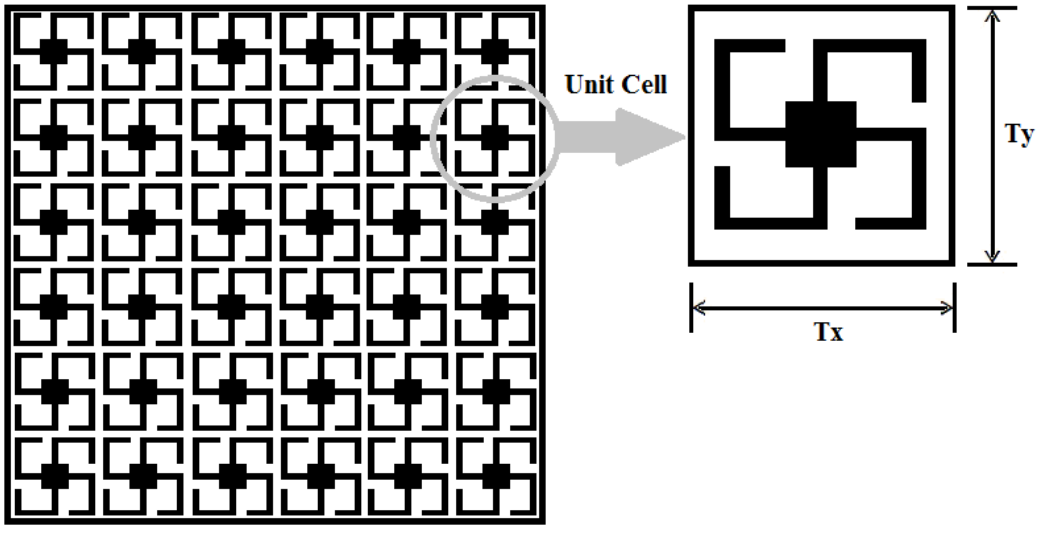

Fig. 1: Front (superior) view of a FSS and its unit cell.

In some FSS applications a wideband frequency response is preferred; however in other applications a multiband frequency response is desired. This question of operating bandwidth is an important problem in FSS theory. Usually, FSS consisting of elements which has a simple shape will produce a single resonance response. To obtain a FSS structure with multiband or wideband frequency response there are many methods such as combined elements, complex elements, including spiral and fractal, multilayered FSS, and the combination of several of those techniques [4-10].

FSS has a long history of research and development and has been investigated over the years for a wide variety of applications. It has been used as radomes and subreflectors integrated with antennas systems, this last one is applied to separate electromagnetic waves into different frequency bands. FSS structures have been successfully proven as a mean to increase the communication capabilities of satellite applications (Voyager, Galileo and Cassini, for example) [1-3].

Applications using FSS in 60 GHz millimeter-wave range have been special attention in the last years, an electronically switchable single layer FSS for 60 GHz applications is presented in [11], this design is based on modified elliptical patch geometry with a single GaAs PIN diode that switches between transparent and opaque modes of operation. A novel millimeter-wave cascaded FSS for de-multiplexing four atmospheric remote sensing bands is presented in [12]. An active FSS using cantilever switches for 60 GHz pass-band switching applications is presented in [13]. A MEMS enable FSS for 60 GHz applications is described in [14], in this case the transmission through the structure can be switched by 30 dB at resonance by switching the MEMS between ON and OFF states, each unit cell has two MEMS contact type switches across the aperture at an 180º interval.

In this paper, a single band-stop FSS with elements geometry based on the concept of simple combined element (SCE), is proposed. The SCE concept uses two or more traditional elements into a single element in each unit cell in particular condition, and providing an explicit relationship between the resonance frequencies, in terms of transmission or reflection coefficient, of combined element FSS [7]. A structure of the element in the unit cell provides similar transmission characteristics for both X-polarized electric field (TE Mode) and for Y-polarized electric filed (TM Mode) for a normal incidence. The dielectric substrate used was the Rogers RO3003, with 0.13 mm of height and relative permittivity equal to 3 and unit cell periodicity (*Tx* = *Ty*) equal to 3.5 mm.

II. ANALYSIS AND FSS STRUCTURE

In the theoretical analysis, the electromagnetic fields must satisfy the periodicity requirements imposed by Floquet's theorem [15].

The wave equation solution is given by [15]:

$$\psi_{pq} = \exp\left[-j(U_{pq}x + V_{pq}y + W_{pq}z)\right] \tag{1}$$

Where:

$$U_{pq} = k\sin\theta\cos\phi + 2\pi p/T_x \tag{2}$$

$$V_{pq} = k\sin\theta\sin\phi + 2\pi q/T_y - 2\pi p/(T_x\tan\alpha) \tag{3}$$

For $p, q = 0, \pm 1, \pm 2, \ldots, \pm\infty$.

$$W_{pq} = \begin{cases} k^2 - T_{pq}^2, & for\, k^2 > T_{pq}^2 \\ -j\left|(k^2 - T_{pq}^2)^{1/2}\right|, & for\, k^2 < T_{pq}^2 \end{cases} \tag{4}$$

With,

$$T_{pq}^2 = U_{pq}^2 + V_{pq}^2 \tag{5}$$

Where p and q are the grating harmonics related to the periodicity present in the FSS. $\vec{k}$ is the propagation vector and θ is the angle between $\vec{k}$ and the normal to the plane of FSS, ϕ is angle between the x axis and the projection of $\vec{k}$ on the x-y plane.

The mode functions for the transverse electric field components can be expressed in terms of the scalar wave function ψ and the resulting TE and TM mode functions, respectively, transverse with respect to the *z* axis, are given as [15]:

$$\vec{\Phi}_{pq}^{TE} = \frac{1}{(T_x T_y)^{1/2}} \left(\frac{V_{pq}}{T_{pq}} \hat{x} - \frac{U_{pq}}{T_{pq}} \hat{y} \right) \psi_{pq} \tag{6}$$

$$\vec{\Phi}_{pq}^{TM} = \frac{1}{(T_x T_y)^{1/2}} \left(\frac{U_{pq}}{T_{pq}} \hat{x} + \frac{V_{pq}}{T_{pq}} \hat{y} \right) \psi_{pq} \tag{7}$$

The modal impedances are related with transverse electric ad magnetics fields as [15]:

$$\eta_{pq}^{TE} = \frac{k}{W_{pq}} \left(\frac{\mu_0}{\varepsilon_0} \right)^{1/2} \tag{8}$$

$$\eta_{pq}^{TE} = \frac{k}{W_{pq}} \left(\frac{\mu_0}{\varepsilon_0} \right)^{1/2} \tag{9}$$

Electromagnetic plane waves can be decomposed into a combination of *E*- and *H*-polarized plane waves that correspond to the TE and TM Floquet modes with both *p*, q = 0, a plane wave with unit electric field intensity incident in the ϕ plane and at an oblique angle θ with the FSS can be given as [15]:

$$\vec{E}^{i} = \sum_{r=1}^{2} A_{00r} \vec{\Phi}_{00r} \tag{10}$$

$$\vec{H}^{i} = \sum_{r=1}^{2} \frac{A_{00r}}{\eta_{00r}} \left(\hat{z} \times \Phi_{00r} \right) \tag{11}$$

A_{00r} is the magnitude of incident filed component and *r* = 1 or 2 is used to designate the TE and TM Floquet modes, respectively. The scattered fields can be expressed in terms of reflection coefficients R_{pq} [15]:

$$\vec{E}^{S} = \sum_{p} \sum_{q} \sum_{r=1}^{2} R_{pqr} \vec{\Phi}_{pqr} \tag{12}$$

$$\vec{H}^{S} = -\sum_{p} \sum_{q} \sum_{r=1}^{2} \left(\frac{R_{pqr}}{\eta_{pqr}} \right) \left(\hat{z} \times \Phi_{00r} \right) \tag{13}$$

The reflection coefficient can be expressed as [15]:

$$R_{pqr} = \eta_{pqr} \iint_{plate} \hat{z} \times \vec{H}^{S} \cdot \Phi_{pqr}^{*} da \tag{14}$$

Φ_{pqr}^{*} is the complex conjugated of Φ_{pqr}. The transmission coefficient can be computed using (14), from the relation between reflection and transmission coefficients.

The proposed structure is based on a simple modification on the element obtained by the SCE concept, where two or more simple or basic elements are combined to obtain a new unique element from the join of these first. Fig. 2 shows the process to form the combined element using SCE. The basic elements: square loop, cross-dipole and square patch were used to obtain this element.

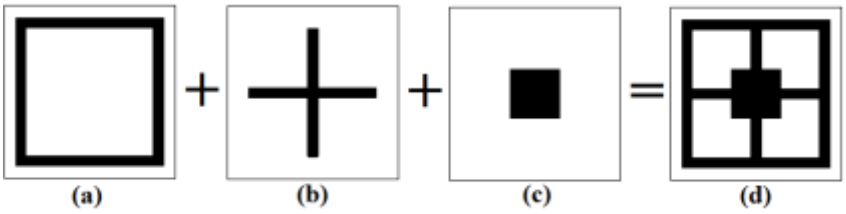

Fig. 2: Unit Cells and its elements: (a) square loop, (b) cross-dipole, (c) square patch and (d) combined element.

A simple change in the combined element was done to obtain the proposed element for the FSS structure, Fig. 3 shows the proposed element and its parameters.

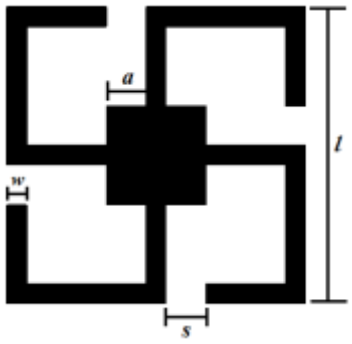

Fig. 3: Proposed element.

The modification consists of small slots (*s*) inserted in the equivalent part of the square loop presented in the combined element, as shown in the previous figure.

III. RESULTS

To investigate the performance of the proposed FSS with modified combined element, in terms of transmission characteristics, the structures were simulated, and the results will be presented in the next figures. Fig. 4 shows the transmission characteristics for the simple elements used to obtain the combined element.

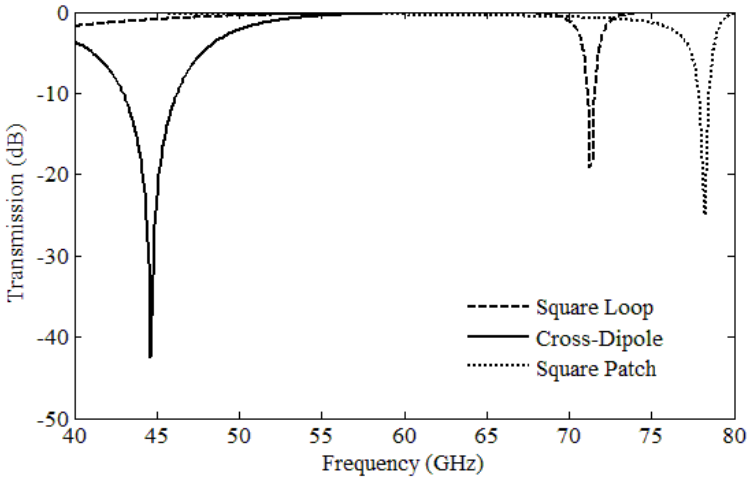

Fig. 4: Transmission coefficients for the simple elements FSS.

In Fig. 4 can be observed the individual results for the three simple elements used as the base to obtain the combined element. For the square loop FSS, can be observed the resonance frequency at 71.25 GHz (-19.12 dB), it has a bandwidth equals to 490 MHz, from 71.01 GHz to 71.50 GHz for a 10 dB insertion loss reference level. In the case of cross-dipole FSS, it is possible to observe a bandwidth equals to 3.34 GHz, approximately,

from 42.93 GHz to 46.27 GHz for a 10 insertion loss reference level, with resonance frequency at 44.63 GHz (-42.53 dB). The square patch FSS presents a resonance frequency at 78.25 GHz (-25.08 dB) and bandwidth equals to 630 MHz, from 77.89 GHz to 78.52 GHz.

Fig. 5 shows the transmission characteristics for the combined element FSS (Fig. 2 (d)). For this case, the results present a resonance frequency at 40 GHz (-46.02 dB) and a bandwidth equals to 20.74 GHz, from 30 GHz to 50.74 GHz. It is possible to observe, in this case, a significant increase in terms of bandwidth when compared to the results obtained for each one individual FSS structure with the simple elements. Another important observation regarding the results, for the transmission coefficient, is that the combined element FSS structure is operating with polarization independence, that is, the same transmission coefficient for both TE and TM modes (X and Y polarized, respectively) for a normal incidence.

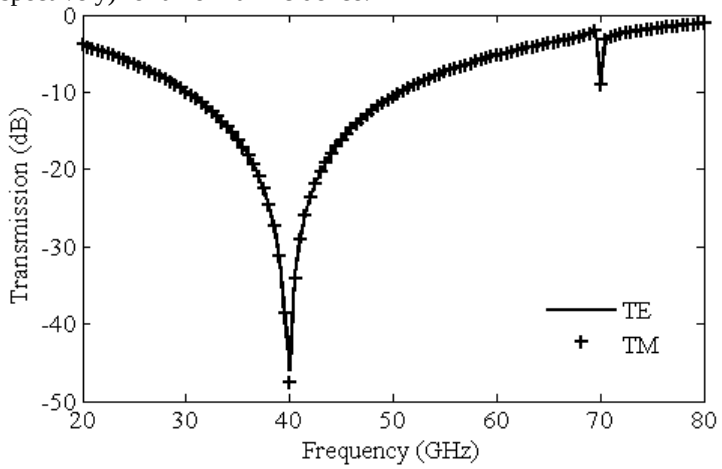

Fig. 5: Transmission coefficient for the combined element FSS.

The transmission characteristics for the proposed FSS with a modification in the combined element are presented in Fig. 6. The proposed FSS parameters used to obtain the results was a = 0.4 mm, w = 0.2 mm, l = 3mm and s = 0.2 mm.

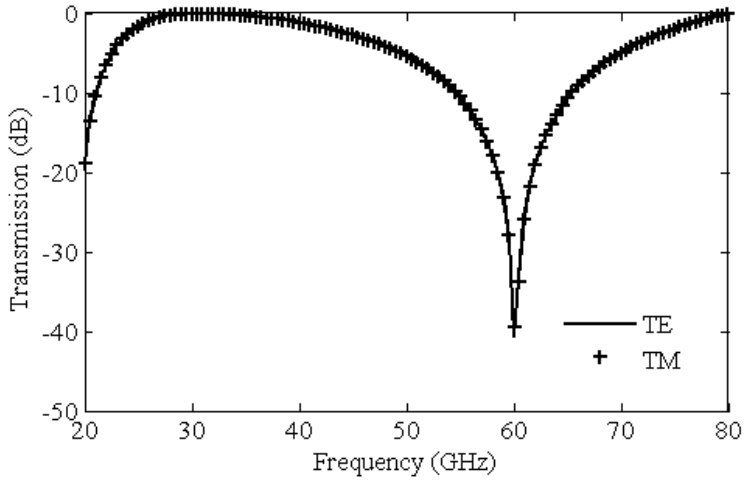

Fig. 6: Transmission coefficient for the proposed FSS.

The results for the proposed FSS presents a resonance frequency at 60 GHz (-40.78 dB), exactly. It has 11.06 GHz of bandwidth, from 54.5 GHz to 65.56 GHz for a 10 dB insertion loss reference level. The slots inserted in to obtain the proposed structure were able to increase the resonance frequency by 20 GHz when compared to the same parameter obtained for the combined element FSS. It is also possible to observe structure operation with polarization independence, the same results for TE and TM modes.

The proposed structure can be used in important applications. The use of the proposed structure in wireless communication technology operating under the 60 GHz frequency band, based on the IEEE 802.11 ad standard, may be mentioned as an example. The millimeter-wave band, especially the unlicensed spectrum at the 60 GHz frequency, is at the spectral frontier of high-bandwidth commercial wireless communication systems. The 60 GHz technology holds great potential to upgrade wireless link throughput to Gbps level. The IEEE 802.11 ad standard has important characteristics, some of them are: operating frequency range at 60 GHz ISM Band, maximum date rate of 7 Gbps, typical distances up to 10 meters and 2.16 GHz of bandwidth. Depending on geographic location the WLAN system uses frequencies located between 57 GHz and 66 GHz. The ITU-R recommends the use of four channels with centre frequencies at 58.32, 60.48, 62.64 and 64.80 GHz [16-18]. Fig 7 shows the transmission characteristics for the proposed structure and the bandwidth used in the 802.11 ad standard for a centre frequency at 60 GHz. It is possible to observe that the prosed FSS can be used for WLAN applications in this frequency range, the bandwidth from 54.5 GHz to 65.56 GHz obtained with the proposed structure fully covers the required band of 2.16 GHz.

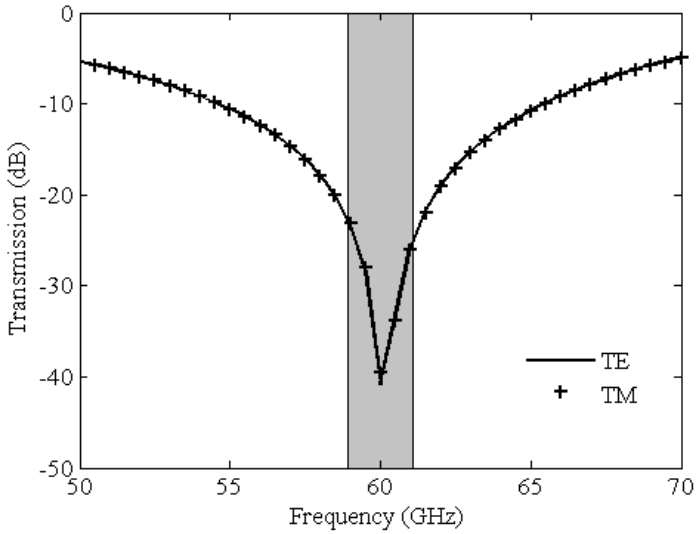

Fig. 7: Transmission coefficient (50-70 GHz) of the proposed FSS, with the bandwidth detail for the application.

IV. CONCLUSION

A compact band-stop FSS is proposed in this paper. A simple modification on a traditional simple combined element FSS was made to obtain the proposed structure, small slots (*s*) was inserted into the SCE element. This process makes it possible to obtain a structure for 60 GHz WLAN (802.11 ad) applications. This FSS structure has the advantage of polarization independent for a normal incidence and wideband, for a 10 dB insertion loss reference level, in the millimeter-wave WLAN frequency applications.

REFERENCES

[1] T. K. Wu, *Frequency selective surface and grid array* (New York, NI: John Wiley & Sons, 1995).

[2] B. A. Munk, *Finite Antenna Array and FSS* (New York, NI: John Wiley & Sons, 2003).

[3] B. A. Munk, *Frequency Selective Surfaces – Theory and Design* (New York, NI: John Wiley & Sons, 2000).

[4] R. Sivasamy, B. Moorthy, M. Kanagasabai, J. V. George, L. Lawrance and D. B. Rajendran, Polarization-independent single-layer ultra-wideband frequency-selective surface, *International Journal of Microwave and Wireless Technologies*, *9(1)*, 2017, 93-97.

[5] R. B. Moreira, A. F. Santos and R. H. C. Maniçoba, A Compact and Stable Frequency Selective Surface for WLAN Applications, *International Journal of Computer Applications*, 166(7), 2017, 1-3.

[6] R. H. C. Maniçoba, A. F. Santos, A. V. Lovato, N. M. Oliveira-Neto, D. B. Brito, A. L. P. S. Campos and A. G. d'Assunção, Numerical Investigation of Multilayer Fractal FSS, *International Journal of Modern Engineering Research*, *4(5)*, 2014, 24-30.

[7] M. Lv, M. Huang, J. Huang, and Z. Wu, Study on the Dual-band Characteristic of Combined Element Based Frequency Selective Surfaces, *Proc. of 2009 IEEE Workshop on Antenna Technology*, Santa Monica, CA, 2009, 1-4.

[8] H. Li and Q. Cao, Design and Analysis of a Controllable Miniaturized Triband Frequency Selective Surface, *Progress In Electromagnetics Reserach Letters*, *52*, 2015, 105-112.

[9] M. Huang, M. Lv, Jun Huang, and Z. Wu, A New Type of Combined Element Multiband Frequency Selective Surface, *IEEE Transactions on Antennas and Propagation*, *57(6)*, 2009, 1798-1803.

[10] D. S. Wang, P. Zhao and C. H. Chan, Design and Analysis of a High-Selectivity Frequency-Selective Surface at 60 GHz, *IEEE Transactions on Microwave Theory and Techniques*, *64(6)*, 2016, 1694-1703.

[11] G. Augustin, B. P. Chacko and T. A. Denidni, Electronically Tunable Frequency Selective Surface at 60 GHz for Beam-Steering Applications, *Proc. of 2015 IEEE International Symposium on Antennas and Propagation & USNC/URSI National Radio Science Meeting*, Vancouver, BC, 2015, 884-885.

[12] J. Poojali, S. Ray, B. Pesala, K. C. Venkata, and K. Arunachalam, Quad band Polarization Insensitive Millimeter Wave Frequency Selective Surface for Remote Sensing, *IEEE Antennas and Wireless Propagation Letters*, *16*, 2017, 1796-1799.

[12] A. Kesavan, B. P. Chacko, and T. A. Denidni, Active Frequency Selective Surfaces using Cantilever Switches for 60-GHz applications, *Proc. of 2015 IEEE International Symposium on Antennas and Propagation & USNC/URSI National Radio Science Meeting*, Vancouver, BC, 2015, 882-883.

[14] G. I. Kiani, T. S. Bird, and K. Y. Chan, MEMS Enabled Frequency Selective Surface for 60 GHz Applications, *Proc. of 2011 IEEE International Symposium on Antennas and Propagation (APSURSI)*, Sopkane, WA, 2011, 2268-2269.

[15] C. C. Chen, Scattering by a two-dimensional periodic array of conducting plates, *IEEE Transactions on Antennas and Propagation*, *18(5)*, 1970, 660-665.

[16] S. Sur, V. Venkateswaran, X. Zhang and P. Ramanathan, 60 GHz Indoor Networking through Flexible Beams: A Link Level Profiling, *Proc. of the 2015 ACM SIGMETRICS International Conference on Measurement and Modeling of Computer Systems*, Portland, OR, 2015, 71-84.

[17] T. Nitsche, C. Cordeiro, A. B. Flores, E. W. Knightly, E. Perahia and J. C. Widmer, IEEE 802.11ad: directional 60 GHz communication for multi-Gigabit-per-second Wi-Fi, *IEEE Communications Magazine*, *52(12)*, 2014, 132-141.

[18] R. C. Daniels, J. N. Murdock, T. S. Rappaport, and R. W. Heath, Jr., 60GHz Wireless: Up Close and Personal, *IEEE Microwave Magazine*, *11(7)*, 2010, 44-50.